PNAS NEXUS

PNAS Nexus, 2025, 4, pgaf186
https://doi.org/10.1093/pnasnexus/pgaf186
Advance access publication 6 June 2025
Research Report

Alpine ice core record of large changes in dust, sea-salt, and biogenic aerosol over Europe during deglaciation

Michel Legrand[a,b,*], Joseph R. McConnell[c], Susanne Preunkert[b,d], David Wachs[d], Nathan J. Chellman[c], Kira Rehfeld[e], Gilles Bergametti[a], Sophia M. Wensman[c], Werner Aeschbach[d], Markus K. Oberthaler[f] and Ronny Friedrich[g]

[a]Université Paris Cité and Univ Paris Est Creteil, CNRS, LISA, Paris F-75013, France
[b]Institut des Géosciences de l'Environnement (IGE), Université Grenoble Alpes, CNRS, Grenoble F-38058, France
[c]Division of Hydrologic Sciences, Desert Research Institute, Reno, NV 89512, USA
[d]Institute of Environmental Physics (IUP), Heidelberg University, Heidelberg D-69120, Germany
[e]Geo- and Environmental Research Center (GUZ), University of Tübingen, Tübingen D-72076, Germany
[f]Kirchhoff-Institute for Physics, Heidelberg University, Heidelberg D-69120, Germany
[g]Curt Engelhorn Centre for Archaeometry, Radiocarbon Laboratory, Mannheim D-68159, Germany
*To whom correspondence should be addressed: Email: michel.legrand@lisa.ipsl.fr
Edited By Barbara Romanowicz

Abstract

Aerosol radiative forcing is an important but often poorly understood component of regional climate. While glacier ice contains the most detailed archives of past atmospheric aerosol composition and temperature, no well-preserved ice records extending into the last climatic transition have been reported for the historically important European region. Here, we use an Alpine ice core to document changes in European aerosols and climate from the end of the last glacial age (LGA) through the Holocene. The core was drilled on a glacier dome in the French Alps called the Dôme du Goûter (DDG), and it provides a stratigraphically intact record of aerosol and climate extending to at least 12 kyears (ky) before present. Although dating near the base of the glacier is not well constrained, the oldest DDG ice layers reflect glacial conditions in western Europe during the LGA. In addition to changes in atmospheric transport, increased sea-salt and dust deposition in western Europe recorded in the LGA ice suggest enhanced westerly winds and more active dust sources, possibly including North Africa. Deposition of terrestrial biogenic indicators during the cold LGA climate was lower, however, consistent with strongly reduced European vegetation. The DDG record of terrestrial biogenic emissions also suggests a decline of European forests throughout the Holocene, resulting from deterioration of climatic conditions and more recently from establishment of the first agricultural societies. The pronounced changes in atmospheric aerosol recorded in Alpine ice imply large variations in aerosol radiative forcing in western Europe during the last 12 ky.

Keywords: Alpine ice core, Holocene, Younger Dryas, dust and sea salt, biotic aerosol

Significance Statement

Aerosol radiative forcing is an important driver of regional climate, so understanding changes in atmospheric aerosol is critical for accurate climate modeling. Although glacier ice contains the most detailed records of past atmospheric aerosol, no ice core records extending to the end of the last climatic transition ~11,700 years ago have been reported for the historically important European region. Here, we report an ice core record collected from the French Alps that spans the last great climatic transition. This record shows increased sea-salt and dust concentrations over western Europe during cold climates consistent with enhanced westerly winds and larger dust emissions possibly from the Sahara, but lower concentrations of biogenic particles during cold climates implying markedly reduced European vegetation cover.

Introduction

Atmospheric aerosols, as well as trace gases, play key roles in radiative transfer, carbon cycling, and climate. Glacier ice is unique in that it simultaneously archives information on past soluble and insoluble aerosol, trace gases, and temperature. As a result, polar ice core records have been used extensively to study past environmental conditions over multiple climate cycles (100 kyears [ky]) at hemispheric and global scales (1–4). Greenland ice has revealed enhanced concentrations of sea-salt and crustal dust aerosol during cold climates compared with the Holocene at high northern latitudes that have been attributed to strengthened westerlies and enhanced dust emissions from

Competing Interest: The authors declare no competing interests.
Received: May 22, 2025. **Accepted:** May 29, 2025

Eastern Asia, respectively (2). Because of the short atmospheric lifetime of aerosols (days to weeks), ice core records proximal to emissions sources can provide information about radiative transfer and environmental conditions on regional scales, in addition to the hemispheric perspective from polar ice core records.

Numerous records of past climate have been derived from European sedimentary archives such as peat, loess, speleothems, and lake sediments (5). However, archives of past atmospheric aerosol extending back to the last climatic transition are available only for a few trace elements (6), largely restricted to water-insoluble aerosol species. Understanding environmental changes and drivers of European climate, such as variations in sea salt and both natural and anthropogenic dust and vegetation emissions, is of particular interest given the magnitude of population growth and extensive land-use change during the rise of Western Civilization under the relatively stable climate of the Holocene following the last glacial/interglacial transition.

Although cores extracted from high-elevation glaciers offer the possibility of documenting past environments in nonpolar regions, most records are restricted to present climate conditions. Except for two ice cores extracted from the Andes (7) and the Tibetan Plateau (8), no glacial records with intact climate–aerosol information other than from high-latitude sites such as those on the polar sheets extend back to the last glacial–interglacial transition (11.65–19.0 ky before present [BP]). While radiocarbon analyses of particulate organic carbon ($PO^{14}C$) have indicated that Pleistocene ice is sometimes present in the bottom layers of West European glaciers (9), it was shown that the climate information has been strongly modified after snow deposition. For example, the $\delta^{18}O$ temperature record from a Colle Gnifetti (CG, Swiss-Italian Alps) core indicated a depletion of 4‰ near the bottom of the core. Although similar to the $\delta^{18}O$ drop observed in Greenland ice during the last climate transition, this change occurred in CG ice dated by ^{14}C measurements to 3 ky BP (9). It was proposed that this large discrepancy resulted from postdepositional liquid migration of ^{18}O at the grain boundary of ice located in zones of strong strain-rate gradients above the inclined bedrock (10).

Here, we report on an Alpine ice core drilled at the flat summit of Dôme du Goûter (DDG) (4,304 m above sea level [asl]) (Fig. S1) located just above the Col du Dome (CDD) ice coring sites (11). In contrast to other Alpine ice cores typically collected from topographic saddles, the DDG bottom ice is less affected by strong strain-rate gradients. We show that $\delta^{18}O$ in the ice decreased in bottom layers covering the late glacial period as indicated by layer thinning-based extrapolation of ^{14}C dating of early Holocene ice, strongly suggesting that the stratigraphically intact climate record extends to ~12 ky BP. Based on this assumption and using analyses of various aerosol proxies including sodium (Na), calcium (Ca), chloride (Cl), aluminum (Al), iron (Fe), phosphorus (P), cerium (Ce), and insoluble particles, we document and discuss changes of sea-salt, dust, and biogenic aerosols emitted by vegetation in response to past climatic conditions in Europe. Free of postdepositional alterations, this Alpine ice record provides an important new climate archive that fills the gap of paleoatmospheric data in this region. These new aerosol and water isotope records are compared to similar extracted from Greenland ice cores representing high northern latitude regions.

Results and discussion

The DDG ice core dating and the $\delta^{18}O$ record

In the following, ages BP are presented as years before 1950 Common Era (CE). The 38.58-m-long (27.5 m water equivalent [mwe]) DDG ice core was dated mainly based on radiocarbon analysis of particulate organic carbon isotopes ($PO^{14}C$) in 12 ice samples. Furthermore, atom trap trace analyses of ^{39}Ar (Materials and methods) in air bubbles of five ice samples were used to date the upper DDG layers for which uncertainties in ^{14}C are relatively high (Fig. 1). Although ^{39}Ar analysis previously was used successfully to date glacier ice (12, 13), this is the first time that the combination of ^{39}Ar and ^{14}C has been used to obtain a full chronology for an alpine ice core. Dating of the upper 22 mwe of the DDG core is very consistent when anchored with the lead perturbation centered at 22.0 mwe (i.e. at ~2 ky BP) attributed to emissions from Roman-era mining and smelting previously detected in ice from the nearby CDD drill site (14) (Fig. S2) and in European peat sediments (6).

Reliable ^{14}C-based age measurements were achieved over the Holocene above 26.3 mwe (9.40 ± 0.26 ky BP) when carbon concentrations in the ice were sufficiently high. Below 26.3 mwe, a Nye parameterization fit to the six ^{14}C measurements between 21.7 and 26.3 mwe (~2.2 to ~9.4 ky BP) (Supporting Text S1 and Fig. S3) was used to account for the strong ice layer thinning of the deepest layers of the glacier frozen to bedrock (15) to allow the dating to extend to the bottom of the core. The DDG ice record indicates an average $\delta^{18}O$ content that remained close to −13‰ down to 26.7 mwe, dropping to −19‰ at ~27.0 mwe (Fig. 2). To evaluate the extrapolated chronology below 26.3 mwe, we compared the DDG $\delta^{18}O$ record in age to more reliably dated climate proxy records from nearby and Greenland (Fig. 3). Applying ages derived from the Nye parameterization, such changes of $\delta^{18}O$ in the DDG ice above ~27.0 mwe are in good agreement with other European archives (Fig. 3), suggesting that the DDG ice is stratigraphically intact as far back as the mid to late Younger Dryas (YD) at 11.65 ky BP (19), i.e. down to 27.0 mwe which comprises ~97% of the current ice thickness (27.8 mwe, Materials and methods) covered by the DDG core. This is the first observed consistency between ^{14}C dating and the $\delta^{18}O$ decline to glacial climate conditions in an Alpine ice core and strongly suggests the absence of any postdepositional effects on the DDG record down to 27.0 mwe.

In contrast, below ~27.0 mwe (i.e. for ice older than ~12 ky BP), there is little agreement between the DDG $\delta^{18}O$ record and the other climate proxy records, suggesting folding and/or faulting effects near the bed. For instance, the climate warming during the Bølling–Allerød (BA) is not fully reflected in our $\delta^{18}O$ record (Fig. 3). However, the water isotope values in this deepest ice are much lower than during the Holocene (remaining close to the minimum value at 12 ky BP) and so generally consistent with cold climate conditions during the late glacial age (LGA) period. As a result, in the following we assume that (i) aerosol concentrations from ice below 27.0 mwe are older than ~12 ky BP and generally representative of LGA conditions in Europe and (ii) the aerosol records in ice younger than ~12 ky BP are stratigraphically intact and extend from the mid- to late YD through the late Holocene.

A number of climate records imply a Holocene Climate Optimum in the Alps during the 10 to 5 ky BP period but often with different timing (5). Unlike Greenland ice records that show a well-marked Climate Optimum (17), other records from the Alps such as the Ammersee ostracod (18) and the Hölloch Cave speleothem (5) $\delta^{18}O$ records are similar to the DDG $\delta^{18}O$ record and show little or no evidence of a Holocene Climate Optimum (Fig. 3).

Using the isotope sensitivity of 1.7‰/°C previously derived for high-elevation Alpine sites (10, 20), the 5‰ difference in $\delta^{18}O$

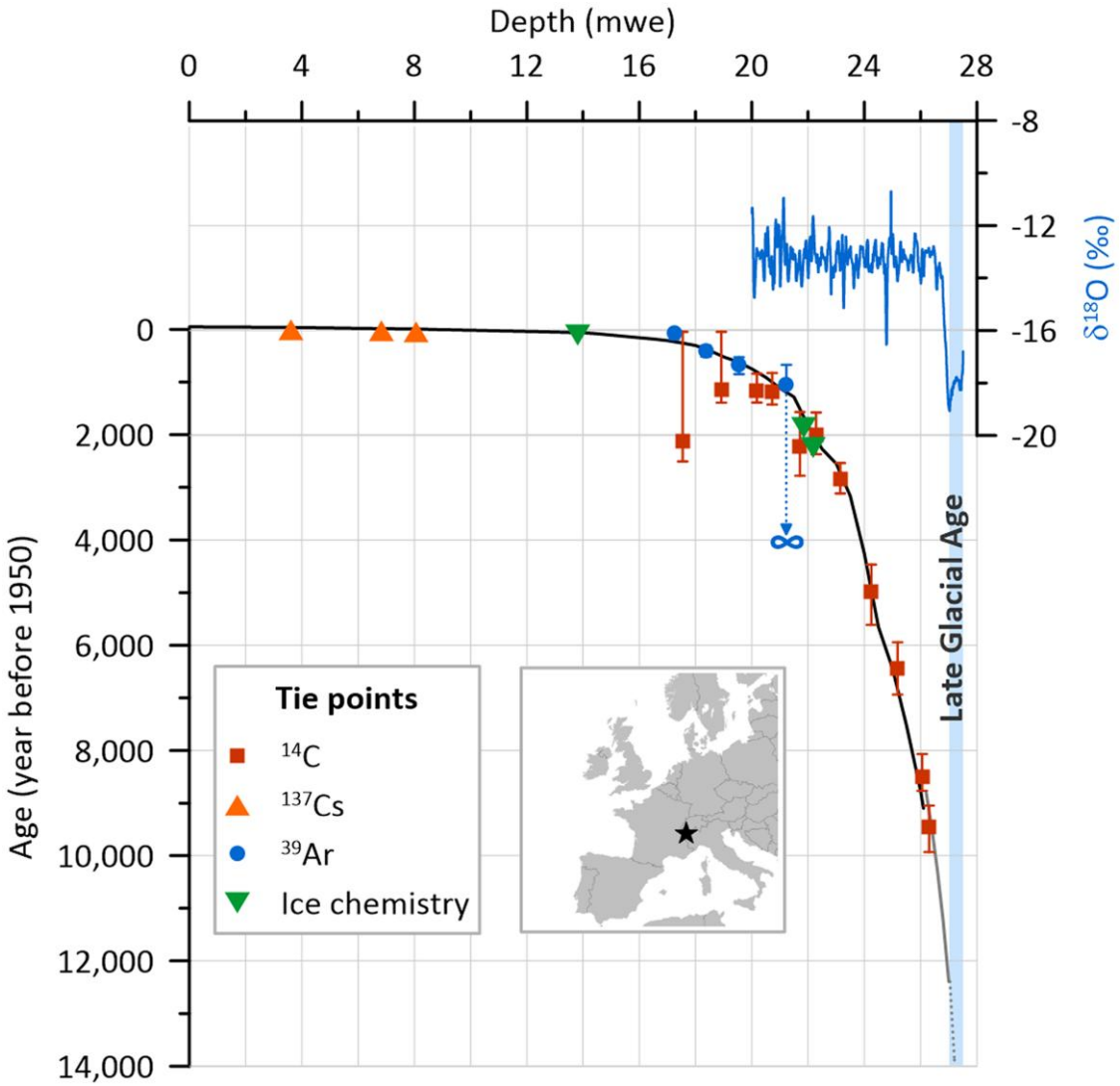

Fig. 1. Holocene dating of the DDG ice core. Top: deeper part of the DDG $\delta^{18}O$ record (0.02 mwe resolution) (in ‰ relative to Standard Mean Ocean Water). Bottom: depth (in meter water equivalent) vs. age relation model (in years before 1950 CE). Dating is based on ^{14}C and ^{39}Ar measurements and various tie points including distinct changes in heavy metals at the onset of the industrial period (~1890 CE) and during antiquity. The solid dark and light lines are the depth age from a Bayesian model and a Nye model, respectively (Supporting Text S1). The dotted light line denotes where the layering is lost with the Nye model. ^{14}C and ^{39}Ar errors are reported as 1 SD. The vertical shaded band indicates the part of the ice core that is not accurately dated but relates to LGA conditions. Inset shows the location of the DDG and CDD drill sites (star).

between Holocene and LGA in DDG ice translates to a temperature decrease of ~3 °C. Evaluation of DDG during the 20th century against nearby seasonally resolved CDD ice records shows that DDG ice consists primarily of summer snow because of strong wintertime wind erosion (Materials and methods; Table S2). Summer temperature reconstructions based on pollen records from western Europe (21) and timberline changes in the Alps (5) indicate summer temperature decreases of 2 and 3.5 °C, respectively. Climate model simulations (22) suggest that the YD in western Europe was characterized by a 6 °C drop of annual temperature compared with warm climate conditions, with a winter and summer half-year decreases of 10 and 2 °C, respectively. Thus, the DDG changes of $\delta^{18}O$ between 26.7 and 27.0 mwe are thus consistent with proxy- and model-based summer temperature reconstructions in western Europe during the last climatic transition.

The long duration of the DDG record enables evaluation of European environmental conditions from the LGA (though not precisely dated) through the Holocene. In our evaluation, we assumed that changes in chemical concentrations in the DDG ice are associated mainly with variations in aerosol deposition, with such variations resulting from both changes in emissions and atmospheric transport between source regions and the Alps. We further assumed that aerosol deposition processes did not change appreciably. Although precipitation rates and thus aerosol atmospheric lifetimes may have varied, the relatively short 1- to 3-day aerosol transport times between potential source regions and the Alps mean they likely had limited impacts on ice concentrations. Note that this is different for Greenland with longer transport times (typically 6 to 10 days) between source regions and the ice sheet (2).

The spatial representativeness of chemical signals archived in DDG ice

To assess year-round and seasonal source regions for aerosols measured in the nearby CDD ice cores, previous studies used the atmospheric aerosol transport and deposition model

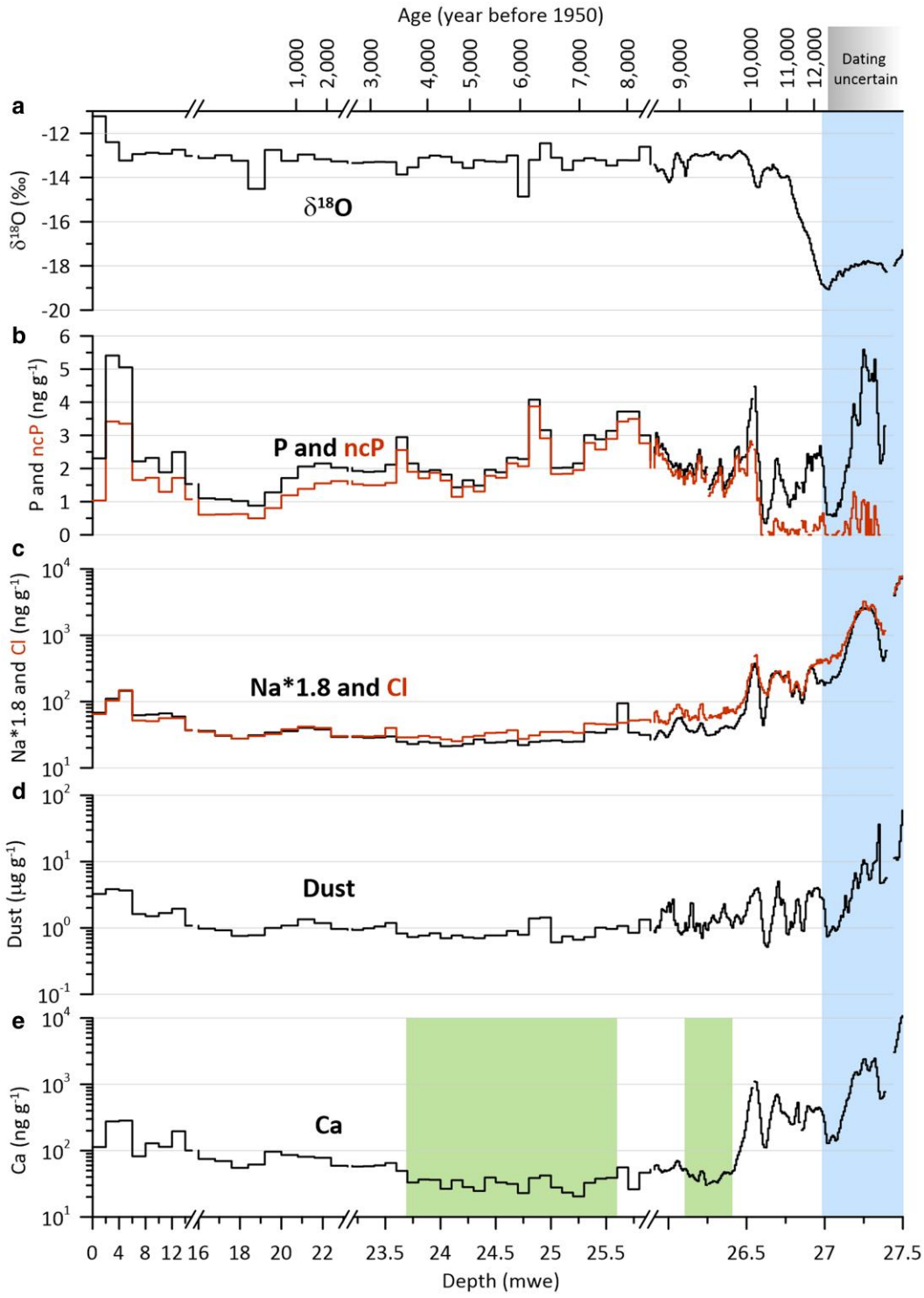

Fig. 2. DDG ice core record of $\delta^{18}O$ ratios and selected chemical species. a) $\delta^{18}O$ (in ‰ relative to SMOW), b) P and ncP (Supporting Text S2), c) Na scaled by 1.8 and Cl, d) dust, and e) Ca concentrations. The 1.8 factor refers to the Cl/Na mass ratio in seawater. Note the use of log scales for Ca, Na, and Cl concentrations. To account for ice layer thinning, the averaging depth intervals were reduced progressively down the core, 2.0 mwe down to 16 mwe depth, 0.8 mwe between 16 and 23.2 mwe depth, 0.1 mwe between 23.2 and 25.9 mwe depth, and 0.02 mwe below 25.9 mwe depth. Changes of averaging depth intervals are shown by breaks in the x-axis. The vertical shaded band below 27.0 mwe refers to the LGA period. The two other shaded bands on the Ca profile indicate time periods with values <50 ng g^{-1} that coincide with previously identified humid Holocene time periods in Sahara (16).

FLEXPART. It was shown that during the 20th century, summertime aerosol concentrations at the remote CDD site mainly reflect aerosol emissions into the boundary layer over regions located within ~1,000 km around the Alps (particularly from France, Italy, and Spain) for various aerosols including submicron particles related to combustion (14, 23) as well as micron-sized particles emitted from soils and vegetation (24). The site is thus representative of aerosol emissions from western Europe.

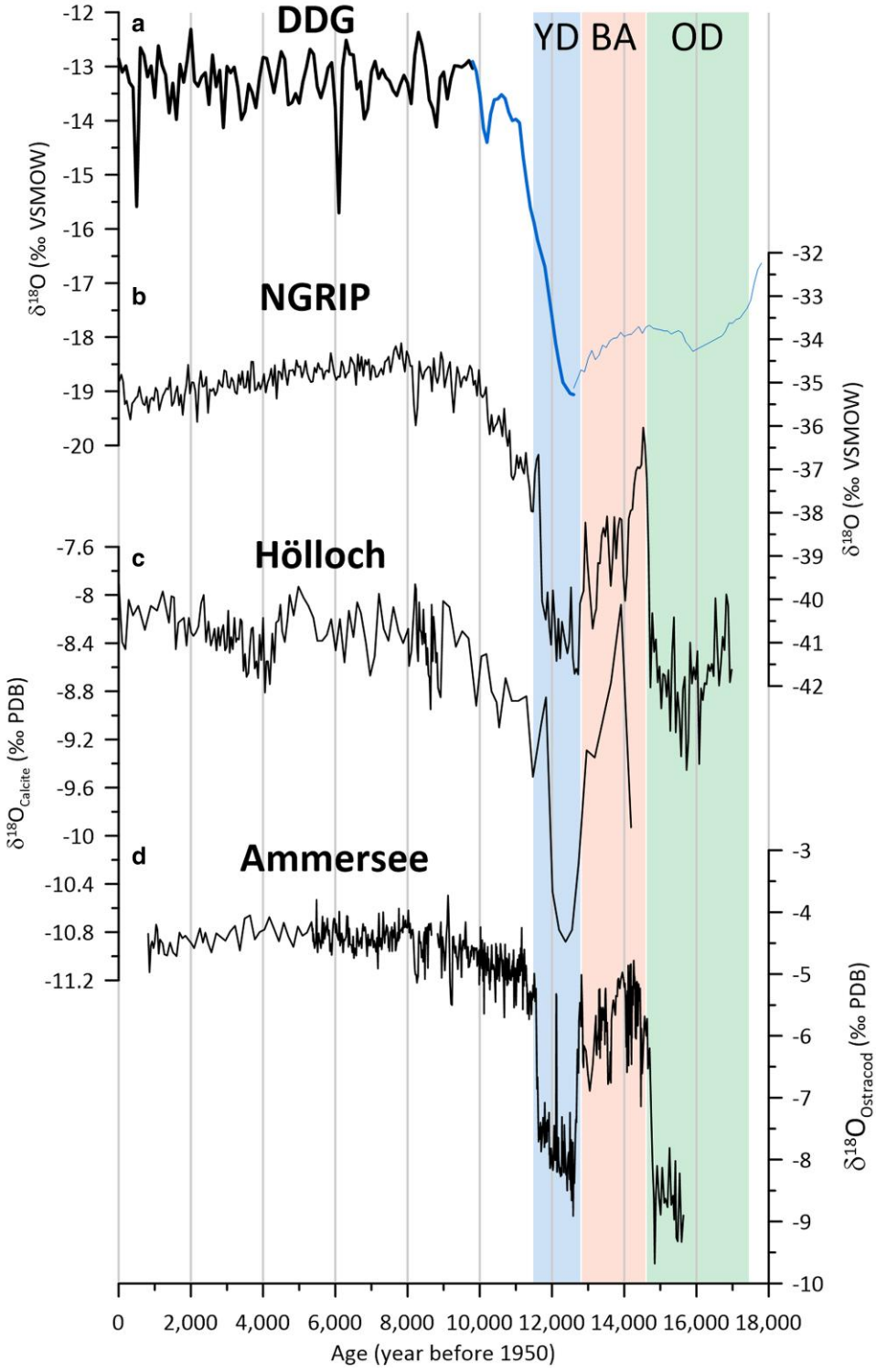

Fig. 3. Comparison between a) the DDG $\delta^{18}O$ record (100-yr smoothing average) and records from b) the Greenland NGRIP (17), c) the speleothem record from Hölloch Cave (5), and d) the ostracod record from Ammersee (18). The two ice records are expressed in in ‰ relative to SMOW; the latter two in % relative to the Peedee Belemnite (PDB) calcite reference. The shaded bands denote the climatic stages of the last glacial age: YD, BA, and OD. The thin line of the bottom DDG $\delta^{18}O$ record denotes the ice layers for which the dating becomes uncertain.

The record of terrestrial biogenic aerosol since the LGA

Biotic particles are thought to modify cloud microphysics at least at continental scales (25). At the global scale, biotic particles emitted by vegetation represent the main natural atmospheric source of noncrustal phosphorus (ncP) (26). Concentrations of ncP in DDG ice calculated using Ce as proxy of the crustal fraction (Supporting Text S2) were low during the LGA, increased 5-fold during the early to mid-Holocene, and then decreased steadily into the late Holocene (Fig. 2). The low ncP concentrations prior to 12 ky BP are in agreement with primarily nonarboreal vegetation cover in western Europe just before the onset of the Holocene (27), with

the rapid ncP increase at ~10 ky BP consistent with forest development in response to improved climatic conditions (temperature and moisture) during the early Holocene. NcP concentrations remained high from 10 to 5.5 ky BP in agreement with quantitative forest reconstructions (27) that indicate a maximum in western European forest cover at that time, followed by a decline of forested area during the second part of the Holocene. Whereas deterioration of climate conditions with decreased temperature in northern Europe and decreased moisture in southern Europe was the leading cause underlying the contraction of forested area from 5.5 to prior to 2 ky BP, land-use changes prevailed after 2 ky BP with enhanced farming and deforestation contributing to landscape fragmentation (28, 29). NcP concentrations in DDG ice declined coevally with this post-5.5 ky BP vegetation decrease in western Europe (Fig. 2).

Increase of sea-salt aerosol during the LGA

Sea-salt aerosol directly scatters solar radiation back to space and, because it is water-soluble, affects climate via cloud droplet size and albedo. The Alps are located some 650 km from the coastline of the Atlantic Ocean and the English Channel. FLEXPART simulations of micron-sized particles (24) thus suggested that the CDD site is impacted by sea-salt aerosols emitted over the mid-latitude Atlantic Ocean and the Mediterranean Sea. Na and Cl concentrations in DDG ice were much higher during the LGA than during the Holocene (Fig. 2) and characterized by a Cl/Na mass ratio close to the seawater composition (1.8). This is consistent with atmospheric models that suggest vigorous westerlies during cold climates in the mid-latitudes North Atlantic regions (2, 22), implying both higher sea-salt emissions over oceanic regions and enhanced eastward transport from these regions towards Europe. The two effects also likely reduced remobilization of chloride (as HCl) from sea-salt aerosol after emission.

The difference in sea-salt concentrations during the LGA compared with the Holocene is far greater at DDG (49-fold for Na, Table S3) than in Greenland (6-fold for Na for the YD and up to 10 times higher during the last glacial maximum (LGM at ~23 ky BP (19)) (2). Possible reasons for the smaller relative change in Greenland include (1) a southward shift in the sea-salt source region for Greenland because of topography-related changes in atmospheric circulation linked to the Laurentide ice sheet (30) and (2) an expansion of multiple-year sea ice that lessened local sea-ice emissions (2) during cold climates. The large increase of sea salt in the western European atmosphere during the LGA may have induced a negative radiative forcing at that time compared with the Holocene.

Changes of dust during the LGA and the Holocene

Dust aerosols affect climate both by absorbing and scattering incoming solar radiation and outgoing planetary radiation and by acting as cloud condensation or ice nuclei (31). Model simulations of the radiative effect of enhanced dust during the LGM (32) indeed indicate negative radiative forcing of the LGM climate by dust. The DDG ice record reveals an 8-fold enhancement of insoluble particle during the LGA compared with the Holocene (Table S3). A recent compilation of paleodust deposited at 11 European sites during the Holocene and LGM indicated an LGM/Holocene dust (<10 μm) deposition ratio of 4.4 ± 4.0 (ranging from 0.2 to 13.6) (33). Since dust deposition during the LGM was higher than during the YD or the Older Dryas (OD), the DDG LGA/Holocene dust ratio of ~8 is in the upper range of the paleodust records in Europe. Furthermore, the LGA/Holocene dust ratio in DDG ice exceeds prior climate model experiments which simulate only a doubling of dust deposition between warm and cold climate stages in Europe (31, 32).

The LGA/Holocene dust ratio of 8 at DDG is intermediate between the ratios of 4 and 10 for Al and Ce, respectively (Fig. S4 and Table S3). Conversely, the LGA/Holocene ratio for Ca is 38, a difference that may be explained by increased inputs from Saharan sources with potential marine carbonate contributions during the LGA. The Sahara has been identified as the present-day main source of dust deposited in Europe (34). Consistent with observed recent trends in dust deposition in the Mediterranean Sea, recent trends in Ca deposition in CDD ice (see Fig. 2 for DDG ice) have been attributed to frequent Saharan dust plumes reaching the Alps after 1950 (24). The DDG Holocene record shows low Ca concentrations below 23.7 mwe depth dated at 3.6 ± 0.6 ky BP, except around 26.0 mwe depth dated at 8.8 ± 0.9 ky BP (Fig. 2). These observations coincide (within dating uncertainties) with the greening of the Northwestern Sahara during the early to mid-Holocene, with lacustrine episodes from 4.5 to 7.5 ky BP and 8.0 to 10.5 ky BP separated by an arid period around 8.0 ky BP (16). While the DDG record does not reveal the arid episode at 5.5–6.7 ky BP (16), the increase observed after 3.6 ± 0.6 ky BP (Fig. 2) is consistent with the well-documented severe aridification of North Africa at 3.6–4.0 ky BP (16). These different observations suggest that the Sahara was the source of a significant portion of the dust transported and deposited over western Europe throughout the Holocene.

At latitudes higher than 50°N, glaciogenic insoluble particles formed during the LGA south of the Scandinavian ice sheet were a source of atmospheric dust at least in northern Europe (31). Furthermore, part of the English Channel between France and the British Isles was exposed during the cold climates and, although limited in spatial extent, may have been a significant source of marine carbonate dust aerosol. In addition, various marine records (35), terrestrial palaeohydrological indicators, and proxy records of vegetation changes (16) all suggest more arid conditions over Mediterranean regions including North Africa, Spain, and Italy during cold climates. It has been proposed that atmospheric meridional transport was strengthened at that time, potentially promoting increased dust transport from these regions towards western Europe (35). These latter assumptions, however, partly conflict with recent model simulations, suggesting wetter conditions caused by a shift of the westerlies further south than previously proposed (36–38).

The chemical composition of dust in DDG during the LGA clearly indicates Ca enrichment with respect to other crustal species, specifically high Ca/Al and (Ca + Mg)/Fe mass ratios (Table 1). These ratios were compared with those of potential dust sources including Saharan and Sahelian sediments, marine carbonates that are rich in calcium, and loess deposits in western Europe. Table 1 indicates high Ca/Al and (Ca + Mg)/Fe ratios in Saharan and marine carbonates compared with loess or Sahelian deposits. Whereas the glaciogenic dust source represented an important source at latitudes higher than 50°N, model simulations indicate very limited southward dispersion (31, 43). The simulated low elevation transport of glaciogenic particles implies atmospheric transport over regional distances (43). This is in stark contrast to transport of dust emitted from deserts such as the Sahara that always is associated with uplift that permits dust plumes to reach at least 3–7-km elevation (44, 45).

The 8-fold higher dust concentration in the LGA DDG ice is similar to that observed in Greenland during the YD and half

Table 1. Mass ratios in different soils and sediments compared with DDG ice. Values under parenthesis refer to the range for Sahel and Saharan sediments and soils (Table S5) and for Western European loess (Table S6).

	Ca/Al	Ca/Mg	(Ca + Mg)/Fe
Soils (39)	0.2	3.0	0.5
Mean sediments (39)	0.92	4.7	2.0
Mean loess (40)	0.8	3.7	2.1
Western Europe loess (40)	0.8 ± 0.4^{a} (0.2–1.1)	4.6 ± 2.2^{a} (2.3–6.9)	2.0 ± 1.0^{a} (0.5–2.7)
Sahel sediments (41)	0.20 ± 0.16^{b} (0.1–0.4)	2.3 ± 0.9^{b} (1.4–3.5)	0.5 ± 0.1^{b} (0.4–0.6)
Marine carbonates (42)	4.8	14.5	7.7
Saharan sediments (41)	3.2 ± 1.8^{b} (1.8–6.5)	6.5 ± 1.2^{b} (5.3–8.1)	5.5 ± 3.3^{b} (3.3–11.5)
Holocene DDG ice	0.9 ± 0.4	4.2 ± 2.0^{c}	1.0 ± 0.5^{c}
LGA DDG ice	5.5 ± 3.1	9.1 ± 6.1^{c}	12.0 ± 3.6^{c}

[a]Postdepositional weathering was found to be low to moderate in these sediments (see details in Supporting Text S5).
[b]See details in Table S5.
[c]Ice concentrations of magnesium (Mg) were corrected from the marine contribution (Supporting Text S2).

that during the slightly colder OD stage (46), although source regions were likely somewhat different. It is difficult to further evaluate differences in dust source regions and atmospheric transport pathways at the DDG and Greenland sites, since the origin of dust deposited in Greenland ice during the cold climates remains less clear than previously assumed (see recent discussions for the YD (47) and for the LGM (48)).

Further investigations, including isotopic studies of dust, are needed to confirm our hypothesis that Saharan dust, possibly supplemented by marine carbonates from exposed continental shelves, was responsible for the large Ca enrichment observed in DDG ice deposited during the cold climates. If correct, our conclusions are consistent with near-surface paleohydrological indicators from North Africa (16), but are in partial disagreement with simulated large-scale cold climate atmospheric circulation (22) and associated implications about regional precipitation (36–38), at least during the summer months reflected in the DDG ice record.

Conclusion

Evaluation of new chemical and $\delta^{18}O$ records, together with ^{14}C dating, suggests that, unlike most other alpine ice records, the DDG climate and aerosol records are intact at least during the past 12 ky. This uniquely detailed archive of the mid-northern latitude atmosphere reveals increased sea-salt deposition during the LGA that suggests enhanced westerlies offshore of western Europe. These increases were larger than in Greenland probably because of a southward shift in the sea-salt source region for Greenland linked to the presence of the Laurentide ice sheet. Increases in dust were similar in the Alps and Greenland in response to enhanced aridity during cold climates, but source regions and transport pathways were different. It is unlikely that the East Asian dust sources, which may have driven dust increase in Greenland, also contributed to the observed western European dust increases, and the large Ca enrichment seen in DDG ice possibly implicates enhanced Saharan sources and/or strengthened northward transport. The DDG record of ncP (a proxy of biogenic aerosol) indicates lower deposition during the LGA corresponding to strongly reduced European vegetation. Finally, while biotic aerosol deposition in the Alps decreased steadily from the early to late Holocene in parallel with the reduction of vegetation cover, Ca deposition increased during the last third of the Holocene, possibly reflecting the end of the Sahara greening. These findings are important for cloud microphysics, radiative transfer, and climate modeling at the European scale.

Materials and methods

The DDG ice core

The DDG ice core (40 m long) was drilled in 1999 to near bedrock at the top of the DDG (4,304 m asl), located 250 m from the CDD drill site (4,250 m asl). The upper 1.4 m of the core was damaged during drilling, so the top of the ice core record corresponds to the year 1997 CE. Furthermore, the deepest ice core piece extracted at the depth of 27.5 mwe did not reach the bedrock. Indeed, after extraction of the last ice core, a heating probe was able to further penetrate an additional 0.35 m.

The mean annual temperature is −11 °C at DDG and CDD (49), and summer temperatures rarely exceed 0 °C. As shown in previous studies conducted at nearby CDD (Supporting Text S3), the seasonal cycle characterized by summer maxima has been very well preserved in all chemical parameters throughout the 20th century, demonstrating without a doubt that surface melting and percolation does not occur at CDG, even under the anomalously warm conditions of the late 20th century (50).

Detailed comparisons of the chemical composition of DDG ice with the seasonally resolved CDD records (50) indicate unambiguously that DDG ice consists largely of summer deposits (Table S2). This likely is a result of very efficient wintertime wind erosion at the DDG summit compared with the more sheltered CDD saddle as indicated by stake accumulation measurements at the two sites (51). Slightly greater $\delta^{18}O$ depletion observed in half-year summer (April to September) averages in CDD suggests less preservation of snow at DDG during the coldest conditions in April, early May, and/or late September. For many species, this mid-summer bias meant slightly higher concentrations (up to a factor of 2) in DDG compared with summer CDD that reflect more efficient upward atmospheric transport of aerosol emitted in the boundary layer under mid-summer conditions. Winds probably were as strong or stronger under glacial (either YD or OD or LGM) conditions, so it seems very unlikely that there was better preservation of winter snow. Therefore, a significant and sustained seasonality shift in net accumulation that would complicate interpretation of the ice core chemistry and isotope records seems improbable.

Chemical analysis

The analyses were conducted using the continuous flow ice core system at the Desert Research Institute (52). Longitudinal core samples (section of 3.3×3.3 cm) were melted sequentially. Analytes included Na, Mg, P, S, Cl, Ca, Al, Fe, Ce, and Pb using two inductively coupled plasma mass spectrometers operating in parallel, colorimetric methods for NO_3 and NH_4, and a Picarro

analyzer for $\delta^{18}O$ (52). Detection limits defined as three times the SD of the blank were 0.05, 0.18, 0.08, 0.06, 3.9, 0.24, 0.18, and 0.60 ng g^{-1} for Na, Mg, P, S, Cl, Ca, Al, and Fe, respectively, and 0.75 pg g^{-1} for Ce and Pb. Similarly, detection limits for NO_3 and NH_4 were 0.50 and 0.13 μg g^{-1} (as N), respectively, and 0.15‰ for $\delta^{18}O$. Previous assessments of measurement recovery with the DRI system for which the online acidification during continuous measurements is limited to a few minutes indicated that recovery was close to 100% for largely soluble Na, Mg, Ca, Cl, S, P, and Pb. Recoveries for Ce were ∼60 and ∼20% for Al and Fe, respectively (53). Reassessment of recoveries specifically in LGA and Holocene DDG ice samples was similar. Semiquantitative, size-resolved insoluble particle concentrations nominally ranging from 0.8 to 10.0 μm were measured at high depth resolution using a laser-based Abakus particle counter (54). Detection limits were ∼0.05 μg g^{-1}.

Ice core dating: radiocarbon (^{14}C) analysis of ice and ^{39}Ar of air bubbles

Twelve DDG ice samples of 18 to 55 cm lengths were analyzed for $PO^{14}C$ content as previously done in CDD ice (14). After decontamination, available ice for $PO^{14}C$ analysis was reduced to 133 to 444 g, with each sample containing particulate organic carbon (POC) masses of 1.0 to 13.7 μgC (Table S1). Radiocarbon samples were prepared at the Institut des Géosciences de l'Environnement with the inline filtration-oxidation-unit developed at the Institute of Environmental Physics. The mean mass blank was 0.2 ± 0.02 μgC with a $F^{14}C$ value of 0.59 ± 0.13. Radiocarbon analyses were conducted at the accelerator mass spectrometer facility of the Curt-Engelhorn-Center Archaeometry. Calibration of the single ^{14}C ages was performed using OxCal version 4 (55, 56). Age uncertainties were large in the two upper samples and in the sample of ice located at 26.5 mwe depth (from 4.0 to 36.7 ky BP). The latter resulted from low organic carbon content (Table S1).

Five DDG ice samples were analyzed for ^{39}Ar content by atom trap trace analysis (ATTA) following previously detailed procedures (12, 57). The ATTA method uses the isotope shift of the electronic transitions in atoms to selectively trap very rare noble gas radioisotopes in a magneto optical trap via laser cooling methods, followed by the counting of individual atoms (57). Sample preparation and gas extraction and purification were done at the Institute of Environmental Physics, Heidelberg. Ice samples were combined to yield more than 1 kg of decontaminated ice per ^{39}Ar sample. The measurements on the resulting 0.6 to 1.0 mL of pure Ar were taken at the Kirchhoff-Institute for Physics, Heidelberg, with the ATTA method (see details in Supporting Text S4 and Table S4).

Acknowledgments

The authors thank all colleagues who participated in the 1999 drilling campaigns at DDG and CDG, as well as the 2022 continuous chemical analysis campaign at DRI.

Supplementary Material

Supplementary material is available at *PNAS Nexus* online.

Funding

The ice core drilling operation at DDG was supported by the European Community via contracts ENV4-CT97 (ALPCLIM) and EVK2 CT2001-00113 (CARBOSOL). National Science Foundation grants 1925417, 2102917, and 2117844 to J.R.M. and N.J.C. provided partial support for the analyses and interpretation at DRI. D.W. was supported by the grant AE 93/22-1 of the Deutsche Forschungsgemeinschaft (DFG).

Author Contributions

M.L., S.P., and J.R.M. conceived and supervised the project. J.R.M., N.J.C., and S.M.W. carried out chemical measurements. S.P. contributed to drilling and prepared ^{14}C samples. R.F. performed ^{14}C analysis. D.W. prepared ^{39}Ar samples and conducted the analyses. M.K.O. and W.A. provided funding acquisition and supervision for the ^{39}Ar work. G.B. evaluated weathering of loess. K.R. conducted model simulations. M.L. and J.R.M. wrote the paper. All edited and reviewed the manuscript.

Data Availability

Ice core data are available at NCEI (National Centers for Environmental Information) data base (https://www.ncei.noaa.gov/access/paleo-search/study/39859).

References

1 Greenland Ice-core Project (GRIP) Members. 1993. Climate instability during the last interglacial period recorded in the GRIP ice core. *Nature*. 364:203–207.
2 Schüpbach S, *et al.* 2018. Greenland records of aerosol source and atmospheric lifetime changes from the Eemian to the Holocene. *Nat Commun*. 9:1476.
3 Petit JR, *et al.* 1999. Climate and atmospheric history of the past 420,000 years from the Vostok ice core, Antarctica. *Nature*. 399: 429–436.
4 Wolff EW, *et al.* 2010. Changes in environment over the last 800,000 years from chemical analysis of the EPICA Dome C ice core. *Quat Sci Rev*. 29:285–295.
5 Heiri O, *et al.* 2014. Palaeoclimate records 60–8 ka in the Austrian and Swiss Alps and their forelands. *Quat Sci Rev*. 106:186–205.
6 Shotyk W, *et al.* 1998. History of atmospheric lead deposition since 12,370 C-14 yr BP from a peat bog, Jura Mountains, Switzerland. *Science*. 281:1635–1640.
7 Thompson LG, *et al.* 1995. Late glacial stage and holocene tropical ice core records from Huascarán, Peru. *Science*. 269:46–50.
8 Thompson LG, *et al.* 2022. Use of $\delta^{18}O$atm in dating a Tibetan ice core record of Holocene/Late Glacial climate. *Proc Natl Acad Sci U S A*. 119:e2205545119.
9 Jenk TM, *et al.* 2009. A novel radiocarbon dating technique applied to an ice core from the Alps indicating late Pleistocene ages. *J Geophys Res*. 114:D14305.
10 Keck L. 2001. Climate significance of Alpine ice core stable isotope records [PhD dissertation]. Heidelberg: Inst. für Umweltphysik, Heidelberg University. p. 125. doi: 10.11588/heidok.00001837.
11 Legrand M, *et al.* 2018. Alpine ice evidence of a three-fold increase in atmospheric iodine deposition since 1950 in Europe due to increasing oceanic emissions. *Proc Natl Acad Sci U S A*. 115: 12136–12141.
12 Feng Z, *et al.* 2019. Dating glacier ice of the last millennium by quantum technology. *Proc Natl Acad Sci U S A*. 116:8781–8786.
13 Ritterbusch F, *et al.* 2022. A Tibetan ice core covering the past 1,300 years radiometrically dated with 39Ar. *Proc Natl Acad Sci U S A*. 119:e2200835119.

14 Preunkert S, *et al.* 2019. Lead and antimony in basal ice from Col du Dome (French Alps) dated with radiocarbon: a record of pollution during antiquity. *Geophys Res Lett*. 46:4953–4961.
15 Nye J. 1963. Correction factor for accumulation measured by the thickness of the annual layers in an ice sheet. *J Glaciol*. 4:785–788.
16 Hoelzmann P, *et al.* Palaeoenvironmental changes in the arid and sub arid belt (Sahara-Sahel-Arabian Peninsula) from 150 kyr to present. In: Battarbee RW, Gasse F, Stickley CE, editors. *Past climate variability through Europe and Africa*. Springer Netherlands, Dordrecht, 2004. p. 219–256.
17 Andersen KK, *et al.* 2004. High-resolution record of Northern Hemisphere climate extending into the last interglacial period. *Nature*. 431:147–151.
18 Grafenstein UV, Erlenkeuser H, Brauer A, Jouzel J, Johnsen SJ. 1999. A Mid-European decadal isotope-climate record from 15,500 to 5000 years B.P. *Science*. 284:1654–1657.
19 Waelbroeck C, *et al.* 2019. Consistently dated Atlantic sediment cores over the last 40 thousand years. *Sci Data*. 6:165.
20 Bohleber P, Wagenbach D, Schöner W, Böhm R. 2013. To what extent do water isotope records from low accumulation Alpine ice cores reproduce instrumental temperature series? *Tellus B Chem Phys Meteorol*. 65:20148.
21 Davis BAS, Brewer S, Stevenson AC, Guiot J. 2003. The temperature of Europe during the Holocene reconstructed from pollen data. *Quat Sci Rev*. 22:1701–1716.
22 Schenk F, *et al.* 2018. Warm summers during the Younger Dryas cold reversal. *Nat Commun*. 9:1634.
23 Arienzo MM, *et al.* 2021. Alpine ice-core evidence of a large increase in vanadium and molybdenum pollution in Western Europe during the 20th century. *J Geophys Res*. 126:e2020JD033211.
24 Legrand M, *et al.* 2023. A two-fold increase of phosphorus in alpine ice over the twentieth century: contributions from dust, primary biogenic emissions, coal burning, and pig iron production. *J Geophys Res*. 128:e2023JD039236.
25 Phillips VTJ, *et al.* 2009. Potential impacts from biological aerosols on ensembles of continental clouds simulated numerically. *Biogeosciences*. 6:987–1014.
26 Mahowald N, *et al.* 2008. Global distribution of atmospheric phosphorus sources, concentrations and deposition rates, and anthropogenic impacts. *Global Biogeochem Cycles*. 22:GB4026.
27 Zanon M, Davis BAS, Marquer L, Brewer S, Kaplan JO. 2018. European forest cover during the past 12,000 years: a palynological reconstruction based on modern analogs and remote sensing. *Front Plant Sci*. 9:253.
28 Kaplan JO, Krumhardt KM, Zimmermann N. 2009. The prehistoric and preindustrial deforestation of Europe. *Quat Sci Rev*. 28:3016–3034.
29 Marquer L, *et al.* 2017. Quantifying the effects of land use and climate on Holocene vegetation in Europe. *Quat Sci Rev*. 171:20–37.
30 Pausata FSR, Li C, Wettstein JJ, Kageyama M, Nisancioglu KH. 2011. The key role of topography in altering North Atlantic atmospheric circulation during the last glacial period. *Clim Past*. 7:1089–1101.
31 Mahowald NM, *et al.* 2006. Change in atmospheric mineral aerosols in response to climate: last glacial period, preindustrial, modern, and doubled carbon dioxide climates. *J Geophys Res*. 111:D10202.
32 Claquin T, *et al.* 2003. Radiative forcing of climate by ice-age atmospheric dust. *Clim Dyn*. 20:193–202.
33 Cosentino NJ, *et al.* 2024. Paleo±Dust: quantifying uncertainty in paleo-dust deposition across archive types. *Earth Syst Sci Data*. 16:941–959.
34 Stuut J-B, Smalley I, O'Hara-Dhand K. 2009. Aeolian dust in Europe: African sources and European deposits. *Quat Int*. 198:234–245.
35 Moreno A, *et al.* 2005. Links between marine and atmospheric processes oscillating on a millennial time-scale. A multi-proxy study of the last 50,000 yr from the Alboran Sea (Western Mediterranean Sea). *Quat Sci Rev*. 24:1623–1636.
36 Ludwig P, Schaffernicht EJ, Shao Y, Pinto JG. 2016. Regional atmospheric circulation over Europe during the Last Glacial Maximum and its links to precipitation. *J Geophys Res*. 121:2130–2145.
37 Kuhlemann J, *et al.* 2008. Regional synthesis of Mediterranean atmospheric circulation during the Last Glacial Maximum. *Science*. 321:1338–1340.
38 Rea BR, *et al.* 2020. Atmospheric circulation over Europe during the Younger Dryas. *Sci Adv*. 6:eaba4844.
39 Bowen H. *Trace elements in biochemistry*. Academic Press, New York, 1966.
40 Újvári G, Varga A, Balogh-Brunstad Z. 2008. Origin, weathering, and geochemical composition of loess in southwestern Hungary. *Quat Res*. 69:421–437.
41 Scheuvens D, Schütz L, Kandler K, Ebert M, Weinbruch S. 2013. Bulk composition of northern African dust and its source sediments—a compilation. *Earth Sci Rev*. 116:170–194.
42 Bowen H. *Environmental chemistry of the elements*. Academic Press, London, 1979.
43 Rousseau D-D, *et al.* 2014. European glacial dust deposits: geochemical constraints on atmospheric dust cycle modeling. *Geophys Res Lett*. 41:7666–7674.
44 Bergametti G, *et al.* Present transport and deposition patterns of African dusts to the North-Western Mediterranean. In: Leinen M, Sarnthein M, editors. *Paleoclimatology and paleometeorology: modern and past patterns of global atmospheric transport*. Springer Netherlands, Dordrecht, 1989. p. 227–252.
45 di Sarra A, Di Iorio T, Cacciani M, Fiocco G, Fuà D. 2001. Saharan dust profiles measured by lidar at Lampedusa. *J Geophys Res*. 106:10335–10347.
46 Steffensen JP. 1997. The size distribution of microparticles from selected segments of the Greenland Ice Core Project ice core representing different climatic periods. *J Geophys Res Oceans*. 102:26755–26763.
47 Han C, *et al.* 2018. High-resolution isotopic evidence for a potential Saharan provenance of Greenland glacial dust. *Sci Rep*. 8(1):15582. doi:10.1038/s41598-018-33859-0.
48 Újvári G, *et al.* 2022. Greenland ice core record of last glacial dust sources and atmospheric circulation. *J Geophys Res*. 127(15):e2022JD036597. doi:10.1029/2022JD036597.
49 Gilbert A, Vincent C. 2013. Atmospheric temperature changes over the 20th century at very high elevations in the European Alps from englacial temperatures. *Geophys Res Lett*. 40:2102–2108.
50 Preunkert S, Wagenbach D, Legrand M, Vincent C. 2000. Col du Dome (Mt Blanc Massif, French Alps) suitability for ice-core studies in relation with past atmospheric chemistry over Europe. *Tellus B Chem Phys Meteorol*. 52:993–1012.

51 Vincent C, Vallon M, Pinglot JF, Funk M, Reynaud L. 1997. Snow accumulation and ice flow at Dôme du Goûter (4300 m), Mont Blanc, French Alps. *J Glaciol*. 43:513–521.
52 McConnell JR, *et al.* 2017. Synchronous volcanic eruptions and abrupt climate change ~17.7 ka plausibly linked by stratospheric ozone depletion. *Proc Natl Acad Sci U S A*. 114: 10035–10040.
53 Arienzo MM, McConnell JR, Chellman NJ, Kipfstuhl S. 2019. Method for correcting continuous ice-core elemental measurements for under-recovery. *Environ Sci Technol*. 53:5887–5894.
54 Ruth U, Wagenbach D, Steffensen J, Bigler M. 2003. Continuous record of microparticle concentration and size distribution in the central Greenland NGRIP ice core during the last glacial period. *J Geophys Res*. 108:D3.
55 Bronk Ramsey C. 1995. Radiocarbon calibration and analysis of stratigraphy: the OxCal program. *Radiocarbon*. 37:425–430.
56 Bronk Ramsey C. 2009. Bayesian analysis of radiocarbon dates. *Radiocarbon*. 51:337–360.
57 Lu ZT, *et al.* 2014. Tracer applications of noble gas radionuclides in the geosciences. *Earth Sci Rev*. 138:196–214.